

A HIGHER-ORDER MULTISCALE METHOD FOR THE WAVE EQUATION

FELIX KRUMBIEGEL[†] AND ROLAND MAIER[†]

ABSTRACT. In this paper we propose a multiscale method for the acoustic wave equation in highly oscillatory media. We use a higher-order extension of the localized orthogonal decomposition method combined with a higher-order time stepping scheme and present rigorous a-priori error estimates in the energy-induced norm. We find that in the very general setting without additional assumptions on the coefficient beyond boundedness, arbitrary orders of convergence cannot be expected but that increasing the polynomial degree may still considerably reduce the size of the error. Under additional regularity assumptions, higher orders can be obtained as well. Numerical examples are presented that confirm the theoretical results.

Keywords. Wave equation, multiscale method, theta scheme, higher-order

AMS subject classification. 65M12, 65M60, 35L05

1. INTRODUCTION

Modeling wave propagation through heterogeneous media typically requires a discretization scale that resolves the heterogeneities that are encoded by an oscillatory coefficient in the underlying partial differential equation (PDE). This is particularly challenging if the coefficient varies on a very fine scale $0 < \varepsilon \ll 1$. It is well-known that standard approaches such as the finite element method (FEM) need to be defined on a mesh with mesh size $h < \varepsilon$ to obtain reasonable approximation properties of the corresponding discrete solution, even in a macroscopic sense. To avoid expensive computations on rather fine scales, especially in a time-dependent scenario where a system of equations has to be solved in every time step, specifically designed multiscale methods present an alternative.

Respective approaches for the wave equation are, e.g., presented in [AG11, EHR11] based on the heterogeneous multiscale method [EE03, EE05, AEEV12] or in [OZ17] using so-called gamblets [Owh17, OS19]. Further methods are presented in [OZ08] and [JEG10, JE12] based on suitable global coordinate transformations. Operator-based upscaling for the wave equation is considered in [VMK05, KM06]. The localized orthogonal decomposition (LOD) method is another prominent multiscale approach and constructs coarse-scale spaces with built-in information on the coefficient on finer scales. The method is originally stated in an elliptic setting [HP13, MP14, MP20] and based on the ideas of the variational multiscale method [Hug95, HFMQ98]. It provably works under minimal structural assumptions on the coefficient and allows computations to be localized to patches such that global fine-scale computations can be completely avoided. Previously, the LOD method has been applied to the wave equation combined with, e.g., a Crank–Nicolson scheme [AH17], a leapfrog scheme [PS17, MP19], or a mass-lumped leapfrog scheme [GM23] for the temporal discretization. The approach has also been used in the context of a damped wave equation in [LMP21] or in connection with waves on spatial

Date: December 22, 2023.

networks [GLM23]. For the treatment of space- and time-dependent coefficients with slow variations in time, suitable updates of the spatial discretization are required as studied in [MV22].

In this work, we focus on a multiscale approach in the spirit of the LOD method for the spatial discretization. Aiming for higher-order convergence rates in the multiscale setting, we apply a higher-order variant of the LOD method based on piecewise polynomials up to degree p , which we refer to as the p -LOD method. The method has been proposed in [Mai20, Mai21] based on a gamblet formulation, and was further refined in [DHM23]. When aiming for higher orders in time, there is the need for a suitable time discretization scheme as common methods such as the leapfrog or Crank–Nicolson scheme only achieve second-order rates. Possible methods include the θ -scheme used in [Kar11], see also the previous works [LKD07, KL07], which is a special case of the Newmark scheme [New59], also referred to as Newmark- β method. With an appropriate choice of θ , convergence rates up to fourth order in time can be achieved. Other possibilities involve rewriting the wave equation into a first order formulation and applying higher-order Runge-Kutta schemes as used, e.g., in [GMM15, AM17].

Here, we combine the p -LOD method with the θ -scheme as used in [Kar11]. Interestingly, arbitrarily high convergence rates in space as observed for the elliptic setting with minimal assumptions in [Mai21, DHM23] can only be obtained for smooth coefficients in the context of the wave equation, which is also to be expected from our theoretical investigations. Nevertheless, increasing the polynomial degree turns out to have a positive effect on the size of the error with respect to the number of degrees of freedom, even without additional smoothness assumptions.

The remainder of this paper is structured as follows. In Section 2, we introduce the general setting and the considered multiscale method regarding the spatial and the temporal discretization. In Section 3, stability and error estimates are derived, and numerical examples are presented in Section 4. In particular, we compare our approach with the classical first-order LOD method for the wave equation, as, e.g., considered in [AH17].

2. A HIGHER-ORDER MULTISCALE METHOD

2.1. Model problem. We consider the wave equation with homogeneous Dirichlet boundary conditions

$$(2.1) \quad \begin{aligned} \ddot{u} - \operatorname{div}(A \nabla u) &= f && \text{in } (0, T) \times \Omega, \\ u(0) &= u_0 && \text{in } \Omega, \\ \dot{u}(0) &= v_0 && \text{in } \Omega, \\ u|_{\partial\Omega} &= 0 && \text{in } (0, T), \end{aligned}$$

where $\Omega \subset \mathbb{R}^d$ is a polygonal, convex, bounded Lipschitz domain for $d \in \{1, 2, 3\}$. We assume that $u_0 \in H_0^1(\Omega)$, $v_0 \in L^2(\Omega)$, $f \in L^2(0, T; L^2(\Omega))$ and $A \in L^\infty(\Omega)$ with $\alpha \leq A(x) \leq \beta$ for almost all $x \in \Omega$, where $0 < \alpha \leq \beta < \infty$. Specifically, we have coefficients in mind that can vary on a fine scale $0 < \varepsilon \ll 1$ but a precise dependence on ε is not required. Note that we might as well consider matrix-valued coefficients and more involved boundary conditions, but we restrict ourselves to the case of scalar coefficients and zero Dirichlet boundary conditions to simplify the presentation.

The variational formulation of equation (2.1) reads as follows: we seek a solution $u \in L^2(0, T; H_0^1(\Omega))$ with $\dot{u} \in L^2(0, T; L^2(\Omega))$ and $\ddot{u} \in L^2(0, T; H^{-1}(\Omega))$ such that

$$(2.2) \quad \langle \ddot{u}, v \rangle_{H^{-1}(\Omega) \times H_0^1(\Omega)} + a(u, v) = (f, v)_{L^2(\Omega)}$$

for all $v \in H_0^1(\Omega)$ with $u(0) = u_0$ and $\dot{u}(0) = v_0$ and with the bilinear form $a(u, v) := (A \nabla u, \nabla v)_{L^2(\Omega)}$. Under the above assumptions on the data, the variational formulation has a unique solution, see, e.g., [LM72, Ch. 3].

2.2. Discretization in space. As mentioned above, classical spatial discretizations based on, e.g., the finite element method need to resolve fine-scale features of the coefficient in order to achieve meaningful approximations in the first place. Otherwise, pre-asymptotic effects may be observed; see also the numerical experiments in [GM23]. To obtain reasonable approximations with a moderate amount of degrees of freedom, more involved constructions are necessary. Here, we construct a problem-adapted finite-dimensional subspace of $H_0^1(\Omega)$ following the ideas of [DHM23] based on the earlier work [Mai21] regarding higher-order multiscale approaches in the spirit of the LOD. First, a finite-dimensional polynomial space is set up, which is altered to obtain a conforming construction and lastly the space is tailored to the problem at hand.

Let $\{\mathcal{T}_H\}_{H>0}$ be a family of regular decompositions of Ω into quasi-uniform d -rectangles; cf. [Cia78, Chs. 2 & 3]. For a given mesh size $H > 0$ and a fixed polynomial degree $p \in \mathbb{N}_0$, we define V_H as the space of piecewise polynomials up to coordinate degree p with respect to the mesh \mathcal{T}_H , i.e.,

$$V_H := \{v \in L^2(\Omega) \mid \forall K \in \mathcal{T}_H : v|_K \text{ is a polynomial of coordinate degree } \leq p\}.$$

For any subdomain $S \subset \Omega$, we define the restricted space

$$V_H(S) = \{v \in V_H \mid \text{supp}(v) \subset S\}$$

and denote by $\Pi_H : L^2(\Omega) \rightarrow V_H$ the L^2 -projection onto V_H . That is, Π_H is defined element-wise for $v \in L^2(\Omega)$ by

$$(2.3) \quad ((\Pi_H v)|_K, w)_{L^2(K)} = (v|_K, w)_{L^2(K)}$$

for all $w \in V_H(K)$ and all $K \in \mathcal{T}_H$. Choosing $w = (\Pi_H v)|_K$ as a test function in (2.3), we directly obtain the stability estimate

$$(2.4) \quad \|\Pi_H v\|_{L^2(K)} \leq \|v\|_{L^2(K)},$$

for all $v \in L^2(K)$. Furthermore, there exists a constant $C_{\text{pr}} > 0$ independent of H (but dependent on p) such that

$$(2.5) \quad \|(1 - \Pi_H)v\|_{L^2(K)} \leq C_{\text{pr}} H^k |v|_{H^k(K)};$$

for all $v \in H^k(K)$ with $k \leq p + 1$, where 1 denotes the identity operator on $H^1(K)$; see, e.g., [Sch98, HSS02, Geo03]. Note that the constant C_{pr} scales like $\left(\frac{(p+1-k)!}{(p+1+k)!}\right)^{\frac{1}{2}}$, and specifically for $k = 1$ we have $C_{\text{pr}} \lesssim (p+1)^{-1}$. There also exists a constant $C_{\text{inv}} > 0$ dependent on p such that the inverse estimate

$$(2.6) \quad \|\nabla v_H\|_{L^2(K)} \leq C_{\text{inv}} H^{-1} \|v_H\|_{L^2(K)}$$

holds for $v_H \in V_H$. Summing up the inequalities (2.4)–(2.6), respectively, over all elements of the mesh, each inequality can be generalized to the whole domain Ω with the use of element-wise gradients on the right-hand sides.

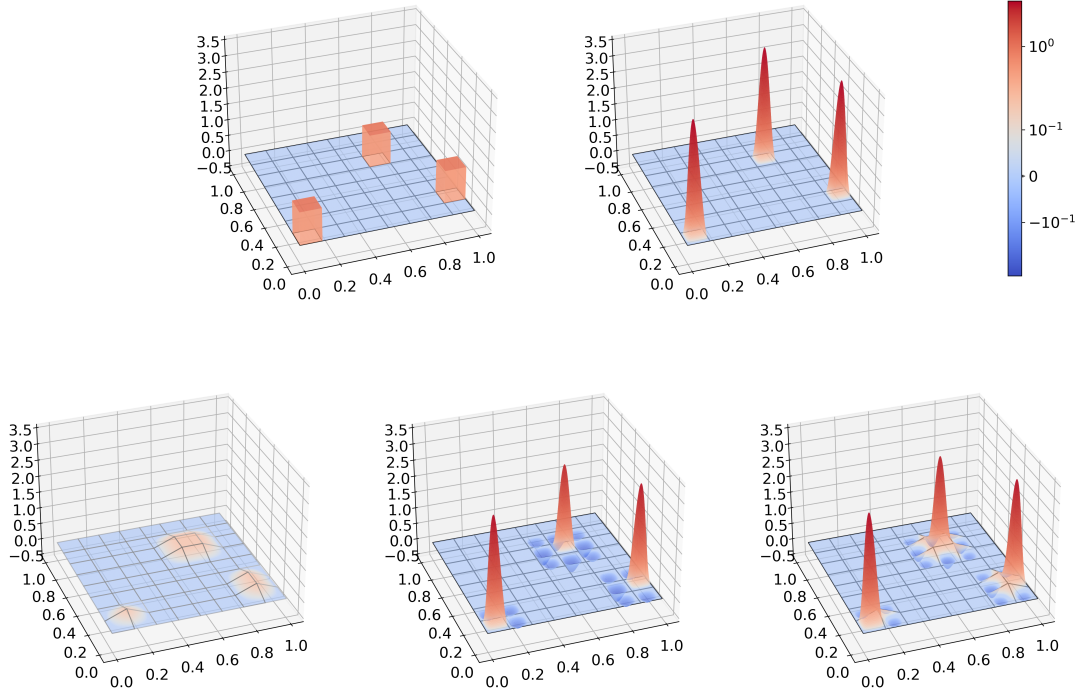


FIGURE 2.1. Plots of different basis functions: three Legendre polynomials $\Lambda_{K,1}$ (top left), the corresponding bubble functions $b_{K,1}$ (top right), the functions ν_K (bottom left), ν_K (bottom middle), and the newly created basis function $\nu_K + \nu_K$ (bottom right).

We denote with $\mathfrak{D} = \bigcup_{K \in \mathcal{T}_H} \{\Lambda_{K,j}\}_{j=1}^M$ for $M = (p+1)^d$ the basis of V_H consisting of tensor-product shifted Legendre polynomials on the element K . While the non-conformity of the space V_H is very beneficial in terms of locality, it complicates the construction of a multiscale space in the spirit of the LOD method. To circumvent the issue while still being able to make use of the locality of V_H , we instead use for each polynomial a certain (local) $H_0^1(K)$ -conforming bubble function, whose L^2 -projection coincides with the polynomial itself. [Mai21, Corollary 3.6] states the existence of functions $\mathfrak{B}' = \bigcup_{K \in \mathcal{T}_H} \{b_{K,j}\}_{j=1}^M$ such that

$$(2.7) \quad b_{K,j} \in H_0^1(K) \quad \text{and} \quad \Pi_H b_{K,j} = \Lambda_{K,j}$$

for each $K \in \mathcal{T}_H$ and $j = 1, \dots, M$. The space $\text{span}(\mathfrak{B}')$ is conforming and has the same dimension as V_H . In the top row of Figure 2.1, three constant Legendre polynomials $\Lambda_{K,1}$ are depicted (left) with their corresponding bubble functions $b_{K,1}$ (right). Note that the depicted bubble functions fulfill the condition (2.7) only for polynomial degrees $p = 0, 1$. For higher polynomial degrees, the bubble functions need to be suitably adjusted, see [DHM23, Rem. 7.1]. The remark also addressed the practical calculation of the bubble functions.

It turns out that the (true) locality of the bubble functions $b_{K,1}$, which approximate the constant Legendre polynomials $\Lambda_{K,1}$ cause problems when constructing a localized multiscale method. Therefore, we suitably extend the support of the corresponding bubble function by one layer of elements without changing its L^2 -projection. Note that this is a

rather technical detail which is discussed and justified in [DHM23] based on the earlier works [AHP21, HP22]. Here we present a practical construction of such extended bubble functions and the corresponding multiscale spaces.

First, we define for a subdomain S the patch of size $k \in \mathbb{N}$ recursively as the set $\mathbf{N}^k(S) = \mathbf{N}^1(\mathbf{N}^{k-1}(S))$, $k > 1$ with $\mathbf{N}^1(S) := \{K \in \mathcal{T}_H \mid \bar{K} \cap \bar{S} \neq \emptyset\}$. Let ι_K for $K \in \mathcal{T}_H$ be such that

$$\iota_K \in V_H^1(\mathbf{N}^1(K)), \quad \iota_K(\hat{x}) = \begin{cases} \frac{1}{2^d}, & \hat{x} \in \bar{K} \setminus \partial \mathbf{N}^1(K), \\ 0, & \hat{x} \in \partial \mathbf{N}^1(K), \end{cases}$$

where V_H^1 refers to the space V_H with the specific choice $p = 1$ and \hat{x} denotes a vertex of the mesh \mathcal{T}_H . Furthermore, for each element $K \in \mathcal{T}_H$ we define ν_K by

$$\nu_K = \sum_{G \in \mathcal{T}_H: G \subset \mathbf{N}^1(K)} \sum_{j=1}^M c_{K,G,j} b_{G,j}, \quad c_{K,G,j} = \int_G (b_{K,1} - \iota_K|_G) \Lambda_{G,j} dx.$$

Further, we define the set of functions

$$\mathfrak{B} = \bigcup_{K \in \mathcal{T}_H} (\{\iota_K + \nu_K\} \cup \{b_{K,j}\}_{j=2}^M),$$

and the corresponding operator $\mathcal{B}_H : V_H \rightarrow \mathcal{B}_H V_H =: U_H$ which is determined by

$$\mathcal{B}_H \Lambda_{K,j} = \begin{cases} \iota_K + \nu_K, & j = 1, \\ b_{K,j}, & j = 2, \dots, M. \end{cases}$$

Note that \mathfrak{B} is a basis of U_H . Furthermore, it holds $\Pi_H(\iota_K + \nu_K) = \Lambda_{K,1}$. We emphasize that $\text{span } \mathfrak{B} \neq \text{span } \mathfrak{B}'$ but $\Pi_H(\text{span } \mathfrak{B}) = \Pi_H(\text{span } \mathfrak{B}') = V_H$, which is a necessary property for the construction below. The plots in the bottom row of 2.1 show examples of the newly created basis functions $\iota_K + \nu_K$ (right) with their respective parts ι_K (left) and ν_K (middle) for the Legendre polynomial and its bubble of the top row. Roughly speaking, the new function $\iota_K + \nu_K$ is composed of a piecewise bilinear continuous part on $\mathbf{N}^1(K)$, which is then adapted by multiple bubbles to fulfill the equality $\Pi_H(\iota_K + \nu_K) = \Lambda_{K,1}$.

Remark 2.1. The construction of the operator \mathcal{B}_H resembles the construction of \mathcal{P}_H in [DHM23] in the sense of $\mathcal{B}_H \circ \Pi_H = \mathcal{P}_H$, such that in particular $\mathcal{B}_H v_H = \mathcal{P}_H v_H$ holds for $v_H \in V_H$, and therefore we get from [DHM23, eq. (3.7)], that there exists a constant $C_b > 0$, which scales with p like $C_b \lesssim (p+1)^2$, such that

$$(2.8) \quad \|\nabla \mathcal{B}_H \Pi_H v\|_{L^2(K)} \leq C_b \|\nabla \Pi_H v\|_{L^2(\mathbf{N}^1(K))}$$

for $v \in L^2(\mathbf{N}^1(K))$ and each element $K \in \mathcal{T}_H$.

Our next step is to define a localized operator \mathcal{C}^ℓ as in [DHM23, Sec. 5.2], that corrects basis functions in a way that the resulting basis has improved approximation properties regarding the underlying multiscale problem. Let $K \in \mathcal{T}_H$, $\ell \in \mathbb{N}$, and define the kernel space $W(\mathbf{N}^\ell(K)) := \ker \Pi_H \cap H_0^1(\mathbf{N}^\ell(K))$. The *element correction* $\mathcal{C}_K^\ell : H_0^1(\Omega) \rightarrow W(\mathbf{N}^\ell(K))$ for $v \in H_0^1(\Omega)$ is then given as the solution $\mathcal{C}_K^\ell v \in W(\mathbf{N}^\ell(K))$ to

$$(2.9) \quad a(\mathcal{C}_K^\ell v, w) = a|_K(v, w)$$

for all $w \in W(\mathbf{N}^\ell(K))$, where $a|_K(v, w) := \int_K A \nabla v \cdot \nabla w dx$ denotes the inner product on $H_0^1(\Omega)$ restricted to the element K . Note that the left-hand side in equation (2.9) is by

definition of the spaces restricted to the patch $\mathbb{N}^\ell(K)$. The *correction operator* is defined as the sum of its local parts, i.e., $\mathcal{C}^\ell = \sum_{K \in \mathcal{T}_H} \mathcal{C}_K^\ell$. If we choose $\ell \in \mathbb{N}$ sufficiently large, such that for each $K \in \mathcal{T}_H$ the left-hand side of (2.9) is global, we formally set $\ell = \infty$ and abbreviate $\mathcal{C} = \mathcal{C}^\infty$. The choice $\ell = \infty$ is optimal in the sense of convergence properties but in practice this operator is cumbersome to deal with due to globally defined element corrections. In practical calculations, it suffices to use the operator \mathcal{C}^ℓ for moderate choices of ℓ instead of \mathcal{C} due to a localization result with exponentially decreasing errors as stated in the following lemma.

Lemma 2.2. ([DHM23, Lem. 5.2]) *There exist constants $C_{\text{loc}}, C_d > 0$ independent of H and ℓ , but dependent on p such that for all $v \in H_0^1(\Omega)$ and $\ell \in \mathbb{N}$ it holds*

$$(2.10) \quad \|\nabla(\mathcal{C} - \mathcal{C}^\ell)v\|_{L^2(\Omega)} \leq C_{\text{loc}} \ell^{\frac{d}{2}} \exp(-C_d \ell) \|\nabla v\|_{L^2(\Omega)}.$$

We are now set to define an appropriate multiscale space. We define

$$\tilde{b}_{K,j}^\ell = \begin{cases} (1 - \mathcal{C}^\ell)(\iota_K + \nu_K), & j = 1, \\ (1 - \mathcal{C}^\ell)b_{K,j}, & j = 2, \dots, M, \end{cases}$$

and the multiscale space $\tilde{U}_H^\ell = \text{span } \tilde{\mathfrak{B}}^\ell$ given by the basis $\tilde{\mathfrak{B}}^\ell = \bigcup_{K \in \mathcal{T}_H} \{\tilde{b}_{K,j}^\ell\}_{j=1}^M$. The basis functions in $\tilde{\mathfrak{B}}^\ell$ are locally supported on $\mathbb{N}^\ell(K)$ for some $K \in \mathcal{T}_H$ (except for $\tilde{b}_{K,1}^\ell$ with support on $\mathbb{N}^{\ell+1}(K)$), and it holds $\Pi_H \tilde{U}_H^\ell = V_H$ with both spaces having the same dimension. The new basis functions include a correction by the problem-dependent operator \mathcal{C}^ℓ such that they achieve better approximation properties for the underlying problem. Analogously to above, we set $\tilde{U}_H = \tilde{U}_H^\infty$ for $\ell = \infty$. Note that the construction of the basis $\tilde{\mathfrak{B}}^\ell$ resembles the construction in [DHM23, Sec. 6], but the presentation here follows a more practical approach. We emphasize that the basis functions $\tilde{b}_{K,j}$ for $j \geq 2$ can be computed from $\Lambda_{K,j}$ directly; see [DHM23]. Thus, only the extended bubble functions $\iota_K + \nu_K$ need actually to be calculated. With the multiscale space \tilde{U}_H^ℓ we are now ready to state our method in the next subsection. First, however, we require some further definitions. We introduce for a series of functions $\{v^n\}_{n=0}^N$ with $v^n \in H^1(\Omega)$ for $n = 0, \dots, N$ the average of two consecutive functions by

$$v^{n+\frac{1}{2}} := \frac{v^{n+1} + v^n}{2},$$

and the first and second discrete time derivatives for such a series and a time step τ by

$$D_\tau v^{n+\frac{1}{2}} := \frac{v^{n+1} - v^n}{\tau}, \quad D_\tau^2 v^n := \frac{v^{n+1} - 2v^n + v^{n-1}}{\tau}.$$

Moreover, we use $a \lesssim b$ if $a \leq Cb$ with a generic constant $C > 0$.

2.3. p -LOD- θ method. The multiscale space \tilde{U}_H^ℓ introduced in the previous subsection can now be used as trial and test space for the variational formulation (2.2) and combined with the θ -scheme as used in [Kar11] to obtain the p -LOD- θ method: find $\tilde{\mathbf{u}}_H^\ell = \{\tilde{u}_H^{\ell,n}\}_{n=0}^N$ with $\tilde{u}_H^{\ell,n} \in \tilde{U}_H^\ell$ for $n = 0, \dots, N$ such that for $n \geq 1$

$$(2.11) \quad \tau^{-2}(\tilde{u}_H^{\ell,n+1} - 2\tilde{u}_H^{\ell,n} + \tilde{u}_H^{\ell,n-1}, \tilde{v}_H)_{L^2(\Omega)} + a(\tilde{u}_H^{\ell,n;\theta}, \tilde{v}_H) = (f^{n;\theta}, \tilde{v}_H)_{L^2(\Omega)}$$

for all $\tilde{v}_H \in \tilde{U}_H^\ell$ and appropriately chosen $\tilde{u}_H^{\ell,0}, \tilde{u}_H^{\ell,1} \in \tilde{U}_H^\ell$, where $\tau = \frac{T}{N}$, $\theta \in [0, \frac{1}{2}]$ is fixed, and the weighted θ -difference is defined by

$$(2.12) \quad \tilde{u}_H^{\ell,n;\theta} = \theta \tilde{u}_H^{\ell,n+1} + (1 - \theta) \tilde{u}_H^{\ell,n} + \theta \tilde{u}_H^{\ell,n-1}.$$

For the right-hand side term f , we have to suitably choose $f^{n;\theta}$. If it is possible to evaluate f pointwise, we define $f^{n;\theta}$ analogously to (2.12) where $f^n = f(n\tau)$. The time discretization is a generalization of multiple schemes, e.g., for $\theta = 0$ we obtain the leapfrog scheme and for $\theta = \frac{1}{4}$ the Crank–Nicolson scheme.

In the following, we show that the error of the p -LOD- θ method applied to the wave equation can be estimated by

$$\max_{0 \leq n < N} \left\| \nabla \left(\tilde{u}_H^{\ell, n+\frac{1}{2}} - u(t_{n+\frac{1}{2}}) \right) \right\|_{L^2(\Omega)} \lesssim H^r + \tau^s,$$

where the spatial convergence rate r depends on the regularity of the initial conditions u_0, v_0 , the right-hand side f , and potentially even the coefficient A . The temporal convergence rate s depends on the choice of θ . For rough heterogeneous coefficients in the elliptic setting, a spatial discretization with the p -LOD method leads a convergence rate of order $r = p + 2$ if the right-hand side is smooth enough, but interestingly this rate cannot be transferred to the wave equation for very rough coefficients, even for smooth data (u_0, v_0, f) . Instead, we find that the order is capped at $r \leq 2$ in the very general setting. The reason is given in Remark 3.14 below based on the theory in Section 3, which is also backed by the numerical examples in Section 4. The order s of the temporal error depends on the choice of θ , we obtain order $s = 2$ if $\theta \neq \frac{1}{12}$ and order $s = 4$ if $\theta = \frac{1}{12}$.

3. STABILITY AND ERROR ANALYSIS

The proof of an error estimate for the p -LOD- θ method is based on energy estimates as in [Chr09, Jol03]. We split the total error of the method into three parts, namely the temporal error, the localization error and the spatial error, which are treated separately. We estimate the errors pointwise in the energy-induced discrete norm $\|D_\tau \cdot\|_{L^2(\Omega)} + \|\nabla \cdot\|_{L^2(\Omega)}$ but emphasize that discrete $L^\infty(0, T; L^2(\Omega))$ -error bounds are also possible (cf. Remark 3.15) with similar techniques as used in [Kar11].

3.1. Energy estimation. In order to show stability of the p -LOD- θ method, we first state the useful property that the discrete energy

$$(3.1) \quad \mathcal{E}^{n+\frac{1}{2}} := \frac{1}{2} \left[\|D_\tau \tilde{u}_H^{\ell, n+\frac{1}{2}}\|_{L^2(\Omega)}^2 + a(\tilde{u}_H^{\ell, n+\frac{1}{2}}, \tilde{u}_H^{\ell, n+\frac{1}{2}}) + \tau^2(\theta - \frac{1}{4})a(D_\tau \tilde{u}_H^{\ell, n+\frac{1}{2}}, D_\tau \tilde{u}_H^{\ell, n+\frac{1}{2}}) \right]$$

is energy-conservative.

Lemma 3.1 (Energy conservation). *The p -LOD- θ method (2.11) conserves the discrete energy (3.1) in the sense that*

$$(3.2) \quad (f^{n;\theta}, \tilde{u}_H^{\ell, n+1} - \tilde{u}_H^{\ell, n-1})_{L^2(\Omega)} = 2(\mathcal{E}^{n+\frac{1}{2}} - \mathcal{E}^{n-\frac{1}{2}}).$$

In particular, for a source term $f \equiv 0$ we obtain energy conservation in the classical sense,

$$\mathcal{E}^{n+\frac{1}{2}} = \mathcal{E}^{n-\frac{1}{2}} = \mathcal{E}^{\frac{1}{2}}.$$

Proof. We choose $\tilde{v}_H = \tilde{u}_H^{\ell, n+1} - \tilde{u}_H^{\ell, n-1}$ as a test function in (2.11) and obtain (3.2) with straight-forward calculations. \square

3.2. Stability. With the energy property (3.2), it suffices to show that the discrete energy of the p -LOD- θ method is positive at all times to obtain stability. Dependent on the choice of θ , we get an unconditionally stable method for $\theta \geq \frac{1}{4}$ and require a CFL condition to ensure stability for $\theta < \frac{1}{4}$.

Theorem 3.2 (Stability). *For $\frac{1}{4} \leq \theta \leq \frac{1}{2}$, the p -LOD- θ method (2.11) is unconditionally stable. For $0 \leq \theta < \frac{1}{4}$, the p -LOD- θ method (2.11) is stable if the CFL condition*

$$(3.3) \quad 1 - (\tau^2(\frac{1}{4} - \theta)\beta(1 + C_{\text{loc}}^2 \ell^d \exp(-2C_d \ell))C_b^2 C_{\text{inv}}^2 H^{-2}) \geq \delta,$$

holds for some $\delta > 0$. In the unconditionally stable case, we formally set $\delta = 1$. In both cases, there exists a constant $C_s > 0$ dependent on δ , α , and β , such that

$$(3.4) \quad \begin{aligned} & \|D_\tau \tilde{u}_H^{\ell, n+\frac{1}{2}}\|_{L^2(\Omega)} + \|\nabla \tilde{u}_H^{\ell, n+\frac{1}{2}}\|_{L^2(\Omega)} \\ & \leq C_s \left(\|D_\tau \tilde{u}_H^{\ell, \frac{1}{2}}\|_{L^2(\Omega)} + \sqrt{\|\tilde{u}_H^{\ell, 1}\|_{L^2(\Omega)} \|\tilde{u}_H^{\ell, 0}\|_{L^2(\Omega)}} \right. \\ & \quad \left. + \tau \sqrt{\theta} \|\nabla D_\tau \tilde{u}_H^{\ell, \frac{1}{2}}\|_{L^2(\Omega)} + \sum_{k=1}^n \tau \|f^{k; \theta}\|_{L^2(\Omega)} \right). \end{aligned}$$

Proof. It is easy to see that $\mathcal{E}^{n+\frac{1}{2}} \geq 0$ for $\theta \geq \frac{1}{4}$. Now, let $\theta < \frac{1}{4}$. Employing the definition of \mathcal{C} , we have

$$a((1 - \mathcal{C})v_H, (1 - \mathcal{C})v_H) = a(v_H, v_H) - a(\mathcal{C}v_H, \mathcal{C}v_H) \leq \beta \|\nabla v_H\|_{L^2(\Omega)}^2.$$

With (2.10), we further estimate

$$(3.5) \quad \begin{aligned} a((1 - \mathcal{C}^\ell)v_H, (1 - \mathcal{C}^\ell)v_H) &= a((1 - \mathcal{C})v_H, (1 - \mathcal{C})v_H) + a((\mathcal{C} - \mathcal{C}^\ell)v_H, (\mathcal{C} - \mathcal{C}^\ell)v_H) \\ &\leq \beta(1 + C_{\text{loc}}^2 \ell^d \exp(-2C_d \ell)) \|\nabla v_H\|_{L^2(\Omega)}^2. \end{aligned}$$

Using (2.9), (2.8), (2.6), and (3.5), we can thus show that the last term in the discrete energy (3.1) is bounded by

$$(3.6) \quad \begin{aligned} & \tau^2(\theta - \frac{1}{4}) a(D_\tau \tilde{u}_H^{\ell, n+\frac{1}{2}}, D_\tau \tilde{u}_H^{\ell, n+\frac{1}{2}}) \\ &= \tau^2(\theta - \frac{1}{4}) a((1 - \mathcal{C}^\ell)\mathcal{B}_H \Pi_H D_\tau \tilde{u}_H^{\ell, n+\frac{1}{2}}, (1 - \mathcal{C}^\ell)\mathcal{B}_H \Pi_H D_\tau \tilde{u}_H^{\ell, n+\frac{1}{2}}) \\ &\leq \tau^2(\theta - \frac{1}{4}) \beta(1 + C_{\text{loc}}^2 \ell^d \exp(-2C_d \ell)) C_b^2 C_{\text{inv}}^2 H^{-2} \|D_\tau \tilde{u}_H^{\ell, n+\frac{1}{2}}\|_{L^2(\Omega)}^2. \end{aligned}$$

Using the CFL condition (3.3) in estimate (3.6) thus yields the positivity of the discrete energy,

$$\mathcal{E}^{n+\frac{1}{2}} \geq \frac{1}{2} a(\tilde{u}_H^{\ell, n+\frac{1}{2}}, \tilde{u}_H^{\ell, n+\frac{1}{2}}) + \frac{1}{2} \delta \|D_\tau \tilde{u}_H^{\ell, n+\frac{1}{2}}\|_{L^2(\Omega)}^2 \geq 0.$$

Next, we show the estimate (3.4). It holds

$$(3.7) \quad \|D_\tau \tilde{u}_H^{\ell, n+\frac{1}{2}}\|_{L^2(\Omega)} + \|\nabla \tilde{u}_H^{\ell, n+\frac{1}{2}}\|_{L^2(\Omega)} \leq \sqrt{2} \max \left\{ \sqrt{\frac{2}{\delta}}, \sqrt{\frac{2}{\alpha}} \right\} \sqrt{\mathcal{E}^{n+\frac{1}{2}}}.$$

To bound the right-hand side term $\sqrt{\mathcal{E}^{n+\frac{1}{2}}}$, we use once again the energy property (3.2) and get

$$\begin{aligned} \mathcal{E}^{n+\frac{1}{2}} - \mathcal{E}^{n-\frac{1}{2}} &= \frac{1}{2} \tau (f^{n; \theta}, D_\tau \tilde{u}_H^{n+\frac{1}{2}} + D_\tau \tilde{u}_H^{n-\frac{1}{2}})_{L^2(\Omega)} \\ &\leq \frac{1}{\sqrt{2\delta}} \tau \|f^{n; \theta}\|_{L^2(\Omega)} \left(\sqrt{\mathcal{E}^{n+\frac{1}{2}}} + \sqrt{\mathcal{E}^{n-\frac{1}{2}}} \right), \end{aligned}$$

which iteratively leads to

$$(3.8) \quad \sqrt{\mathcal{E}^{n+\frac{1}{2}}} \leq \sqrt{\mathcal{E}^{\frac{1}{2}}} + \sum_{k=1}^n \frac{1}{\sqrt{2\delta}} \tau \|f^{k;\theta}\|_{L^2(\Omega)}.$$

The initial energy $\sqrt{\mathcal{E}^{\frac{1}{2}}}$ can be estimated with (3.1),

$$\sqrt{\mathcal{E}^{\frac{1}{2}}} \leq \frac{1}{\sqrt{2}} \left(\|D_\tau \tilde{u}_H^{\ell, \frac{1}{2}}\|_{L^2(\Omega)} + \sqrt{\beta \|\tilde{u}_H^{\ell, 1}\|_{L^2(\Omega)} \|\tilde{u}_H^{\ell, 0}\|_{L^2(\Omega)}} + \tau \sqrt{\theta \beta} \|\nabla D_\tau \tilde{u}_H^{\ell, \frac{1}{2}}\|_{L^2(\Omega)} \right).$$

Combining this estimate with (3.7) and (3.8), the assertion follows with

$$C_s = \max \left\{ \sqrt{\frac{2}{\delta}}, \sqrt{\frac{2}{\alpha}} \right\} \max \left\{ \frac{1}{\sqrt{\delta}}, \sqrt{\beta} \right\}. \quad \square$$

Remark 3.3. Note that the constants C_b and C_{inv} depend on p , thus the CFL condition depends on p as well. While the theory in [DHM23] predicts a quadratic scaling with respect to p , the practical scaling of the constants appears to be much better.

3.3. Error estimate for the p -LOD- θ method. In this subsection, we present and prove a full error estimate for the p -LOD- θ method. First, we give the general assumptions to obtain the convergence results.

Assumption 3.4. Assume that

- (A0) $f \in C^4([0, T]; H^k(\Omega))$ for some $k \in \mathbb{N}_0$,
- (A1) $u(0) = u_0 \in H_0^1(\Omega)$, $\partial_t u(0) = v_0 \in H_0^1(\Omega)$,
- (A2) $\partial_t^m u(0) := \partial_t^{m-2} f(0) + \text{div} A \nabla (\partial_t^{m-2} u(0)) \in H_0^1(\Omega)$, $m = 2, \dots, 4$,
- (A3) $\partial_t^5 u(0) := \partial_t^3 f(0) + \text{div} A \nabla (\partial_t^3 u(0)) \in L^2(\Omega)$,
- (A4) There exists a constant $C_{\text{init}} > 0$ such that

$$\sum_{m=0}^4 \|\partial_t^m u(0)\|_{H_0^1(\Omega)} + \|\partial_t^5 u(0)\|_{L^2(\Omega)} \leq C_{\text{init}}.$$

Remark 3.5. Assumption 3.4 is also referred to as *well-prepared and compatible of order 4*; cf. [AH17, Def. 4.5]. Under this assumption, we obtain

$$\partial_t^5 u \in C([0, T]; L^2(\Omega)), \quad \partial_t^m u \in C([0, T]; H_0^1(\Omega)), \quad m = 0, \dots, 4,$$

based on the result in [LM72, Ch. 3] applied to the variational formulation (2.2) and its temporal derivatives. Furthermore, we can bound the norms of the solution from above and denote with $C_{\text{data}} > 0$ a generic constant such that

$$\sum_{m=0}^4 \|\partial_t^m u\|_{C([0, T]; H_0^1(\Omega))} + \|\partial_t^5 u\|_{C([0, T]; L^2(\Omega))} \lesssim \|f\|_{C^4([0, T]; H^k(\Omega))} + C_{\text{init}} \leq C_{\text{data}}$$

holds. Note that the assumption (A4) in that context is mainly required to ensure that the corresponding norms do not scale negatively with the oscillation scale on which the coefficient varies.

Assumption 3.4 with $k = 0$ is the most general to show the desired convergence properties of our method. In order to further improve the rates, additional assumptions are required, specifically that $\partial_t^m u \in C([0, T]; H^{j+1}(\Omega))$ for some $j \geq 1$ and $m \in \mathbb{N}$. Again, the conditions can be fulfilled by appropriate assumptions on the initial data, the right-hand side, the domain, and the coefficient. As this is not the target regime of this paper, the corresponding assumptions are presented in Appendix A. In the respective setting, we

can also bound the norms of the solution and its temporal derivatives in their respective norms by a modified constant C_{data} , that then depends on the regularity parameters j, k and corresponding norms of the initial data and right-hand side.

Theorem 3.6 (Error of the p -LOD- θ method). *Assume that Assumption 3.4 holds for some $k \in \mathbb{N}_0$ and additionally let $u \in C^4([0, T]; H^{j+1}(\Omega))$ for some $j \in \mathbb{N}_0$ (we note that the case $j = 0$ is covered by Assumption 3.4). Let $r = \min\{k+1, j+2, p+2\}$ and $\ell \gtrsim r|\log H|$. Further, let $\tilde{\mathbf{u}}_H^\ell = \{\tilde{u}_H^{\ell, n}\}_{n=0}^N$ be the solution to the p -LOD- θ method defined in (2.11) with suitable initial conditions and u the solution to (2.2). Then with $t_n = n\tau$, it holds that*

$$(3.9) \quad \left\| D_\tau \tilde{u}_H^{\ell, n+\frac{1}{2}} - \frac{u(t_{n+1}) - u(t_n)}{\tau} \right\|_{L^2(\Omega)} + \left\| \nabla(\tilde{u}_H^{\ell, n+\frac{1}{2}} - u(t_{n+\frac{1}{2}})) \right\|_{L^2(\Omega)} \lesssim (H^r + \tau^s) C_{\text{data}}$$

with $s = 2$ if $\theta \neq \frac{1}{12}$ and $s = 4$ if $\theta = \frac{1}{12}$.

Before we prove the theorem, we give some auxiliary definitions. First, we introduce the function \tilde{z}_H^ℓ as the solution to the semi-discrete problem

$$(3.10) \quad (\partial_t^2 \tilde{z}_H^\ell(t), \tilde{v}_H^\ell)_{L^2(\Omega)} + a(\tilde{z}_H^\ell(t), \tilde{v}_H^\ell) = (f(t), \tilde{v}_H^\ell)_{L^2(\Omega)}$$

for all $\tilde{v}_H^\ell \in \tilde{U}_H^\ell$ and $t \in [0, T]$ with initial conditions $\tilde{z}_H^\ell(0) = (1 - \mathcal{C}^\ell) \mathcal{B}_H \Pi_H u_0$ and $\partial_t \tilde{z}_H^\ell(0) = (1 - \mathcal{C}^\ell) \mathcal{B}_H \Pi_H v_0$. Analogously to above, we write $\tilde{z}_H = \tilde{z}_H^\infty$ for $\ell = \infty$.

Remark 3.7. Differentiating (3.10) with respect to time and using the regularity of the initial conditions (which follows from Assumption 3.4), we obtain by standard ODE theory that $\partial_t^4 \tilde{z}_H^\ell \in C^2([0, T], \tilde{U}_H^\ell)$ and $\tilde{z}_H^\ell \in C^6([0, T], \tilde{U}_H^\ell)$. Furthermore, we have

$$(3.11) \quad \sum_{k=0}^6 \|\tilde{z}_H^\ell\|_{C^k([0, T]; H_0^1(\Omega))} \leq C_{\text{data}}.$$

Next, we define the operator $\tilde{\mathcal{P}}$ as the orthogonal projection onto the global multiscale space \tilde{U}_H with respect to the bilinear form a , i.e., for $v \in H_0^1(\Omega)$ we define $\tilde{\mathcal{P}}v$ by

$$(3.12) \quad a(\tilde{\mathcal{P}}v, \tilde{v}_H) = a(v, \tilde{v}_H)$$

for all $\tilde{v}_H \in \tilde{U}_H$. Let u be the solution to the variational formulation (2.2) with regularity properties as stated in Remark 3.5 and $\tilde{u}_H^{\ell, n} \in \tilde{U}_H^\ell$ for $\ell \in \mathbb{N}$ and $\tilde{u}_H^n \in \tilde{U}_H$ for $\ell = \infty$ be the solutions to the p -LOD- θ method defined in (2.11) for $n = 0, \dots, N$ with initial conditions defined analogously to [Kar11] by $\tilde{u}_H^{\ell, 0} = \mathbf{u}_0$ and $\tilde{u}_H^{\ell, 1}$ is obtained from

$$(3.13) \quad (\tilde{u}_H^{\ell, 1} - \tilde{u}_H^{\ell, 0}, \tilde{v}_H^\ell)_{L^2(\Omega)} + \tau^2 \theta a(\tilde{u}_H^{\ell, 1} - \tilde{u}_H^{\ell, 0}, \tilde{v}_H^\ell) = \\ \tau(\mathbf{v}_0, \tilde{v}_H^\ell)_{L^2(\Omega)} - \frac{\tau^2}{2} a(\mathbf{u}_0, \tilde{v}_H^\ell)_{L^2(\Omega)} - \frac{\tau^3}{12} a(\mathbf{v}_0, \tilde{v}_H^\ell)_{L^2(\Omega)} + \frac{\tau^2}{2} (f(0), \tilde{v}_H^\ell)_{L^2(\Omega)} \\ + \frac{\tau^3}{6} (\partial_t f(0), \tilde{v}_H^\ell)_{L^2(\Omega)} + \frac{\tau^4}{24} (\partial_t^2 f(0), \tilde{v}_H^\ell)_{L^2(\Omega)}$$

for all $\tilde{v}_H^\ell \in \tilde{U}_H^\ell$, where $\mathbf{u}_0 = (1 - \mathcal{C}^\ell) \mathcal{B}_H \Pi_H u_0$ and $\mathbf{v}_0 = (1 - \mathcal{C}^\ell) \mathcal{B}_H \Pi_H v_0$.

The following lemma provides an estimate for the time discretization error. We make use of the stability estimate (3.4) to derive an error estimate and motivate the choice for the initial conditions (3.13). The ideas in the proof follow [Kar11] with some technicalities related to the p -LOD method.

Lemma 3.8 (Temporal error). *Let $\{\tilde{u}_H^{\ell,n}\}_{n=0}^N$ and \tilde{z}_H^ℓ be the solutions to (2.11) and (3.10), respectively, and let $\zeta^n = \tilde{u}_H^{\ell,n} - \tilde{z}_H^\ell(t_n)$ with $t_n = n\tau$. Then there exists a constant $C_{\text{sd}} > 0$, dependent on $T, \theta, \delta, \alpha$ and β such that*

$$(3.14) \quad \|D_\tau \zeta^{n+\frac{1}{2}}\|_{L^2(\Omega)} + \|\nabla \zeta^{n+\frac{1}{2}}\|_{L^2(\Omega)} \leq \tau^s C_{\text{sd}} C_{\text{data}},$$

where $s = 2$ if $\theta \neq \frac{1}{12}$ and $s = 4$ if $\theta = \frac{1}{12}$.

Proof. The sequence $\{\zeta^n\}_{n=0}^N$ solves

$$(D_\tau^2 \zeta^n, \tilde{v}_H^\ell)_{L^2(\Omega)} + a(\zeta^n; \tilde{v}_H^\ell) = (\partial_t^2 \tilde{z}_H^{n,\ell;\theta}, \tilde{v}_H^\ell)_{L^2(\Omega)} - (D_\tau^2 \tilde{z}_H^\ell(t_n), \tilde{v}_H^\ell)_{L^2(\Omega)}$$

for all $\tilde{v}_H^\ell \in \tilde{U}_H^\ell$ and $n = 1, \dots, N-1$, where $\tilde{z}_H^{n,\ell;\theta}$ is once again defined as in (2.12). Moreover, $\tilde{z}_H^{n,\ell} = \tilde{z}_H^\ell(t_n)$. With the stability estimate (3.4), we therefore obtain

$$(3.15) \quad \begin{aligned} & \|D_\tau \zeta^{n+\frac{1}{2}}\|_{L^2(\Omega)} + \|\nabla \zeta^{n+\frac{1}{2}}\|_{L^2(\Omega)} \\ & \leq C_s \left(\|D_\tau \zeta^{\frac{1}{2}}\|_{L^2(\Omega)} + \sqrt{\|\zeta^1\|_{L^2(\Omega)} \|\zeta^0\|_{L^2(\Omega)}} + \tau \sqrt{\theta} \|\nabla D_\tau \zeta^{\frac{1}{2}}\|_{L^2(\Omega)} \right. \\ & \quad \left. + \sum_{k=1}^n \tau \|\partial_t^2 \tilde{z}_H^{k,\ell;\theta} - D_\tau^2 \tilde{z}_H^\ell(t_k)\|_{L^2(\Omega)} \right). \end{aligned}$$

For the sum in the last row of (3.15), we obtain with a Taylor expansion the estimate

$$(3.16) \quad \sum_{k=1}^n \tau \|\partial_t^2 \tilde{z}_H^{k,\ell;\theta} - D_\tau^2 \tilde{z}_H^\ell(t_k)\|_{L^2(\Omega)} \lesssim \tau^s T \|\tilde{z}_H^\ell\|_{C^{s+2}([0,T];L^2(\Omega))},$$

where $s = 2$ if $\theta \neq \frac{1}{12}$ and $s = 4$ if $\theta = \frac{1}{12}$. Since $\zeta^0 = 0$, the second term on the right-hand side of (3.15) vanishes. It remains to bound the two other terms on the right-hand side. Subtracting the left-hand side of (3.13) from

$$(\tilde{z}_H^\ell(t_1) - \tilde{z}_H^\ell(t_0), \tilde{v}_H^\ell)_{L^2(\Omega)} + \theta \tau^2 a(\tilde{z}_H^\ell(t_1) - \tilde{z}_H^\ell(t_0), \tilde{v}_H^\ell)$$

with the specific test function $\tilde{v}_H^\ell = \frac{\zeta^1 - \zeta^0}{\tau}$ and dividing by τ , we obtain after some straightforward calculations that

$$\begin{aligned} & \|D_\tau \zeta^{\frac{1}{2}}\|_{L^2(\Omega)}^2 + \tau^2 \theta \|\nabla D_\tau \zeta^{\frac{1}{2}}\|_{L^2(\Omega)}^2 \\ & \lesssim \tau^s (\|\tilde{z}_H^\ell\|_{C^5([0,T];L^2(\Omega))} + \|f\|_{C^3([0,T];L^2(\Omega))}) (\|D_\tau \zeta^1\|_{L^2(\Omega)} + \tau \sqrt{\theta} \|\nabla D_\tau \zeta^1\|_{L^2(\Omega)}), \end{aligned}$$

where $s = 2$ if $\theta \neq \frac{1}{12}$ and $s = 4$ if $\theta = \frac{1}{12}$. This yields

$$\|D_\tau \zeta^1\|_{L^2(\Omega)} + \sqrt{\theta} \tau \|\nabla D_\tau \zeta^1\|_{L^2(\Omega)} \lesssim 2\tau^s (\|\tilde{z}_H^\ell\|_{C^{s+1}([0,T];L^2(\Omega))} + \|f\|_{C^{s-1}([0,T];L^2(\Omega))}),$$

and combined with (3.15) and (3.16) we obtain

$$\begin{aligned} & \|D_\tau \zeta^{n+\frac{1}{2}}\|_{L^2(\Omega)} + \|\nabla \zeta^{n+\frac{1}{2}}\|_{L^2(\Omega)} \\ & \leq \tau^s C_{\text{sd}} (\|\tilde{z}_H^\ell\|_{C^{s+2}([0,T];L^2(\Omega))} + \|\tilde{z}_H^\ell\|_{C^{s+1}([0,T];L^2(\Omega))} + \|f\|_{C^{s-1}([0,T];L^2(\Omega))}) \end{aligned}$$

for some $C_{\text{sd}} > 0$. Note that the constant C_{sd} scales linearly with the final time T . Finally, (3.14) follows with Remark 3.7. \square

Remark 3.9 (Initial conditions). If $\theta \neq \frac{1}{12}$, the convergence rate in time in Lemma 3.8 is only $s = 2$ and the initial condition $\tilde{u}_H^{\ell,1}$ do not need to be of fourth order. Therefore, they can be computed by the reduced equation

$$(\tilde{u}_H^{\ell,1} - \tilde{u}_H^{\ell,0}, \tilde{v}_H^\ell) + \tau^2 \theta a(\tilde{u}_H^{\ell,1} - \tilde{u}_H^{\ell,0}, \tilde{v}_H^\ell) = \tau(v^0, \tilde{v}_H^\ell) - \frac{\tau^2}{2} a(u^0, \tilde{v}_H^\ell) + \frac{\tau^2}{2} (f(0), \tilde{v}_H^\ell),$$

where $\tilde{u}_H^{\ell,0}$, u^0 and v^0 are chosen as above; cf. [Kar11]. Note that in this case we require less regularity assumptions on \tilde{z}_H^ℓ and f .

The following lemma quantifies another ingredient of the total error, namely the localization error that investigates the difference of using the correction operator \mathcal{C}^ℓ or the global operator \mathcal{C} . The proof follows ideas presented in [GM23] adjusted to the higher-order setting.

Lemma 3.10 (Localization error). *Let \tilde{z}_H^ℓ and \tilde{z}_H be solutions to (3.10) with appropriate localization parameter, and let $\eta(t) = \tilde{z}_H(t) - \tilde{z}_H^\ell(t)$. Then there exists a constant $C_{le} > 0$ dependent on T , the polynomial degree p , α , and β such that*

$$(3.17) \quad \|D_\tau \eta(t_{n+\frac{1}{2}})\|_{L^2(\Omega)} + \|\nabla \eta(t_{n+\frac{1}{2}})\|_{L^2(\Omega)} \leq C_{le} C_{loc} \ell^{\frac{d}{2}} \exp(-C_d \ell) C_{data}.$$

Proof. Let $z_H(t) = \mathcal{B}_H \Pi_H \tilde{z}_H(t)$ and $z_H^\ell(t) = \mathcal{B}_H \Pi_H \tilde{z}_H^\ell(t)$. Further, define

$$\tilde{e}_H^\ell(t) = (1 - \mathcal{C}^\ell) e_H^\ell(t) = (1 - \mathcal{C}^\ell)(z_H(t) - z_H^\ell(t))$$

and observe that $\tilde{e}_H^\ell(t)$ solves

$$(3.18) \quad \begin{aligned} & ((1 - \mathcal{C}^\ell) \partial_t^2 e_H^\ell(t), \tilde{v}_H^\ell) + a((1 - \mathcal{C}^\ell) e_H^\ell(t), \tilde{v}_H^\ell) \\ &= -(f(t), (\mathcal{C} - \mathcal{C}^\ell) v_H) + ((1 - \mathcal{C}) \partial_t^2 z_H(t), (\mathcal{C} - \mathcal{C}^\ell) v_H) \\ & \quad + ((\mathcal{C} - \mathcal{C}^\ell) \partial_t^2 z_H(t), (1 - \mathcal{C}^\ell) v_H) + a((\mathcal{C} - \mathcal{C}^\ell) z_H(t), (\mathcal{C} - \mathcal{C}^\ell) v_H) \end{aligned}$$

for all $v_H \in U_H$, where $\tilde{v}_H^\ell = (1 - \mathcal{C}^\ell) v_H \in \tilde{U}_H^\ell$. We define an appropriate energy by

$$E(t) := \frac{1}{2} [\|(1 - \mathcal{C}^\ell) \partial_t e_H^\ell(t)\|_{L^2(\Omega)}^2 + a((1 - \mathcal{C}^\ell) e_H^\ell(t), (1 - \mathcal{C}^\ell) e_H^\ell(t))]$$

for all $t \in [0, T]$. We now choose $(1 - \mathcal{C}^\ell) \partial_t e_H^\ell(t)$ as a test function in equation (3.18) and integrate in time. Using (2.8), (2.5), (2.4), (2.10), and the fact that $e_H^\ell(0) = 0$, we obtain after taking the supremum over $t \in [0, T]$

$$(3.19) \quad \begin{aligned} & \sup_{t \in [0, T]} E(t) \\ & \leq [H C_{pr} C_b (\|f\|_{C([0, T], L^2(\Omega))} + T \|\partial_t f\|_{C([0, T], L^2(\Omega))}) \\ & \quad + H C_{pr} C_b (\|\partial_t^2 \tilde{z}_H\|_{C([0, T], L^2(\Omega))} + T \|\partial_t^3 \tilde{z}_H\|_{C([0, T], L^2(\Omega))}) \\ & \quad + H^2 C_{pr}^2 C_b (\|\nabla \partial_t^2 \tilde{z}_H\|_{C([0, T], L^2(\Omega))} + T \|\nabla \partial_t^3 \tilde{z}_H\|_{C([0, T], L^2(\Omega))}) \\ & \quad + \beta C_b^2 C_{loc} \ell^{\frac{d}{2}} \exp(-C_d \ell) (\|\nabla \tilde{z}_H\|_{C([0, T], L^2(\Omega))} + T \|\nabla \partial_t \tilde{z}_H\|_{C([0, T], L^2(\Omega))})] \\ & \quad \cdot C_{loc} \ell^{\frac{d}{2}} \exp(-C_d \ell) \sqrt{\frac{2}{\alpha}} (\sup_{t \in [0, T]} E(t))^{\frac{1}{2}}. \end{aligned}$$

Since we would like to compare the solutions in the different spaces \tilde{U}_H^ℓ and \tilde{U}_H , we use for $v, w \in U_H$ the estimate

$$(3.20) \quad \|(1 - \mathcal{C})v - (1 - \mathcal{C}^\ell)w\|_{L^2(\Omega)} \leq \|(1 - \mathcal{C}^\ell)(v - w)\|_{L^2(\Omega)} + \|(\mathcal{C} - \mathcal{C}^\ell)v\|_{L^2(\Omega)}.$$

More precisely, we consider the specific choices $v = z_H(t)$ and $w = z_H^\ell(t)$ and apply (3.19) to the first term on the right-hand side of (3.20). The second term of (3.20) can be bounded using (2.10). Finally, we obtain (3.17) with Remark 3.7. \square

Remark 3.11. If we choose the localization parameter $\ell \gtrsim r|\log H|$, then the error estimate (3.17) reduces to

$$\|D_\tau \eta(t_{n+\frac{1}{2}})\|_{L^2(\Omega)} + \|\nabla \eta(t_{n+\frac{1}{2}})\|_{L^2(\Omega)} \lesssim H^r C_{\text{data}},$$

which matches the spatial error estimate as investigated below.

To bound the spatial error, we split the error into two parts. The first part describes the error between the semi-discrete solution and the projection of the exact solution into the multiscale space \tilde{U}_H^ℓ . The second part of the spatial error is the error between the exact solution and its projection. We bound the two terms in the following two lemmas.

Lemma 3.12 (Spatial discretization error). *Let \tilde{z}_H and u be the solutions to (3.10) and (2.2), respectively, and let $\tilde{\mathcal{P}}$ be the projection defined in (3.12). Further, let $\varphi(t) = \tilde{z}_H(t) - \tilde{\mathcal{P}}u(t)$ and $\rho(t) = u(t) - \tilde{\mathcal{P}}u(t)$. Then there exists a constant $C_{\text{sdp}} > 0$ (dependent on α) such that*

$$(3.21) \quad \|\partial_t \varphi(t)\|_{L^2(\Omega)} + \|\nabla \varphi(t)\|_{L^2(\Omega)} \leq C_{\text{sdp}} \int_0^t \|\partial_t^2 \rho(s)\|_{L^2(\Omega)} \, ds.$$

Proof. The result follows from [Jol03]. For any $t \in [0, T]$, the function $\varphi(t)$ solves the semi-discrete problem

$$(3.22) \quad (\partial_t^2 \varphi(t), \tilde{v}_H)_{L^2(\Omega)} + a(\varphi(t), \tilde{v}_H) = (\partial_t^2 \rho(t), \tilde{v}_H)_{L^2(\Omega)}.$$

for all $\tilde{v}_H \in \tilde{U}_H$. We define the energy

$$\mathfrak{E}(t) = \frac{1}{2} [\|\partial_t \varphi(t)\|_{L^2(\Omega)}^2 + a(\varphi(t), \varphi(t))],$$

choose $\tilde{v}_H = \partial_t \varphi(t)$ as test function in (3.22), and integrate in time from 0 to t , we obtain

$$\sqrt{\mathfrak{E}(t)} \leq \sqrt{\mathfrak{E}(0)} + \sqrt{2} \int_0^t \|\partial_t^2 \rho(s)\|_{L^2(\Omega)} \, ds.$$

Since $\mathfrak{E}(0) = 0$, this is the assertion. \square

Lemma 3.13 (Projection error). *Let u be the solution to (2.2) and $\tilde{\mathcal{P}}$ the projection defined in (3.12). Further, let $\rho(t) = u(t) - \tilde{\mathcal{P}}u(t)$ and suppose that Assumption 3.4 holds for some $k \in \mathbb{N}_0$. Further, suppose that $u \in C^2([0, T]; H^{j+1}(\Omega))$ for some $j \in \mathbb{N}_0$ and set $r = \min\{j+2, k+1, p+2\}$. Then there exists a constant $C_p > 0$ dependent on the polynomial degree p and α such that*

$$(3.23) \quad \begin{aligned} \|\nabla \rho(t)\|_{L^2(\Omega)} &\leq C_p H^r (\|f\|_{C([0, T]; H^k(\Omega))} + \|\partial_t^2 u\|_{C([0, T]; H^{j+1}(\Omega))}), \\ \|\rho(t)\|_{L^2(\Omega)} &\leq C_p C_{\text{pr}} H^{r+1} (\|f\|_{C([0, T]; H^k(\Omega))} + \|\partial_t^2 u\|_{C([0, T]; H^{j+1}(\Omega))}). \end{aligned}$$

Proof. For any $t \in [0, T]$, we have that $\rho(t) \in \ker \Pi_H$ and combined with (2.5) we obtain

$$\|\rho(t)\|_{L^2(\Omega)} = \|(1 - \Pi_H)\rho(t)\|_{L^2(\Omega)} \leq C_{\text{pr}} H \|\nabla \rho(t)\|_{L^2(\Omega)}.$$

Further, using the orthogonality property of Π_H and (2.5), we have

$$\begin{aligned}
 \alpha \|\nabla \rho(t)\|_{L^2(\Omega)}^2 &\leq a(\rho(t), \rho(t)) = a(u(t) - \tilde{\mathcal{P}}u(t), u(t) - \tilde{\mathcal{P}}u(t)) \\
 &= a(u(t), u(t) - \tilde{\mathcal{P}}u(t)) = (f(t) - \partial_t^2 u(t), u(t) - \tilde{\mathcal{P}}u(t))_{L^2(\Omega)} \\
 (3.24) \quad &= ((1 - \Pi_H)(f(t) - \partial_t^2 u(t)), (1 - \Pi_H)(u(t) - \tilde{\mathcal{P}}u(t)))_{L^2(\Omega)} \\
 &\leq C_{\text{pr}}(H^k \|f(t)\|_{H^k(\Omega)} + H^{j+1} \|\partial_t^2 u(t)\|_{H^{j+1}(\Omega)}) C_{\text{pr}} H \|\nabla \rho(t)\|_{L^2(\Omega)}.
 \end{aligned}$$

Combining both equations gives the desired result. \square

As mentioned above, the error estimate for the full error of the p -LOD- θ method is split into four parts, which we have analyzed above and can now put together to obtain the main result.

Proof of Theorem 3.6. Let $e^n = \tilde{u}_H^{\ell,n} - u(t_n)$. We have

$$(3.25) \quad e^n = \zeta^n - \eta(t_n) + \varphi(t_n) - \rho(t_n),$$

where $\zeta^n = \tilde{u}_H^{\ell,n} - \tilde{z}_H^\ell(t_n)$, $\eta(t) = \tilde{z}_H(t) - \tilde{z}_H^\ell(t)$, $\varphi(t_n) = \tilde{z}_H(t_n) - \tilde{\mathcal{P}}u(t_n)$ and $\rho(t) = u(t) - \tilde{\mathcal{P}}u(t)$ as in the above lemmas. The full error of the p -LOD- θ method can thus be bounded by

$$\begin{aligned}
 \|D_\tau e^{n+\frac{1}{2}}\|_{L^2(\Omega)} + \|\nabla e^{n+\frac{1}{2}}\|_{L^2(\Omega)} &\leq \|D_\tau \zeta^{n+\frac{1}{2}}\|_{L^2(\Omega)} + \|\nabla \zeta^{n+\frac{1}{2}}\|_{L^2(\Omega)} \\
 (3.26) \quad &+ \|D_\tau \eta(t_{n+\frac{1}{2}})\|_{L^2(\Omega)} + \|\nabla \eta(t_{n+\frac{1}{2}})\|_{L^2(\Omega)} \\
 &+ \|D_\tau \varphi(t_{n+\frac{1}{2}})\|_{L^2(\Omega)} + \|\nabla \varphi(t_{n+\frac{1}{2}})\|_{L^2(\Omega)} \\
 &+ \|D_\tau \rho(t_{n+\frac{1}{2}})\|_{L^2(\Omega)} + \|\nabla \rho(t_{n+\frac{1}{2}})\|_{L^2(\Omega)}.
 \end{aligned}$$

Using a Taylor expansion of $D_\tau \varphi(t_{n+\frac{1}{2}})$, Lemma 3.12, and the continuity in time, there exist a $\xi \in [0, t_{n+1}]$ with

$$\|D_\tau \varphi(t_{n+\frac{1}{2}})\|_{L^2(\Omega)} + \|\nabla \varphi(t_{n+\frac{1}{2}})\|_{L^2(\Omega)} \leq 2C_{\text{sdp}} \int_0^{t_{n+1}} \|\partial_t^2 \rho(s)\|_{L^2(\Omega)} \leq 2C_{\text{sdp}} T \|\partial_t^2 \rho(\xi)\|_{L^2(\Omega)}.$$

With a Taylor expansion of $D_\tau \rho(t_{n+\frac{1}{2}})$ and applying Lemma 3.13 (which also holds for $\partial_t \rho(t)$ and $\partial_t^2 \rho(t)$), we get

$$\begin{aligned}
 \|\nabla \rho(t_{n+\frac{1}{2}})\|_{L^2(\Omega)} &\lesssim H^r (\|f\|_{C([0,T];H^k(\Omega))} + \|u\|_{C^2([0,T];H^{j+1}(\Omega))}), \\
 \|D_\tau \rho(t_{n+\frac{1}{2}})\|_{L^2(\Omega)} &\lesssim H^{r+1} (\|f\|_{C^1([0,T];H^k(\Omega))} + \|u\|_{C^3([0,T];H^{j+1}(\Omega))}), \\
 \|\partial_t^2 \rho(\xi)\|_{L^2(\Omega)} &\lesssim H^{r+1} (\|f\|_{C^2([0,T];H^k(\Omega))} + \|u\|_{C^4([0,T];H^{j+1}(\Omega))).
 \end{aligned}$$

Finally, with (3.26), Lemma 3.8, and Lemma 3.10 with $\ell \gtrsim r|\log H|$, we obtain

$$\|D_\tau e^{n+\frac{1}{2}}\|_{L^2(\Omega)} + \|\nabla e^{n+\frac{1}{2}}\|_{L^2(\Omega)} \lesssim (H^r + \tau^s) C_{\text{data}}.$$

Note that the hidden constant depends on the final time T , δ , α , β , and the polynomial degree p and is independent of the mesh size H , the time step size τ , and the scale ε on which the coefficient varies. Note that $s = 2$ if $\theta \neq \frac{1}{12}$ and $s = 4$ if $\theta = \frac{1}{12}$. \square

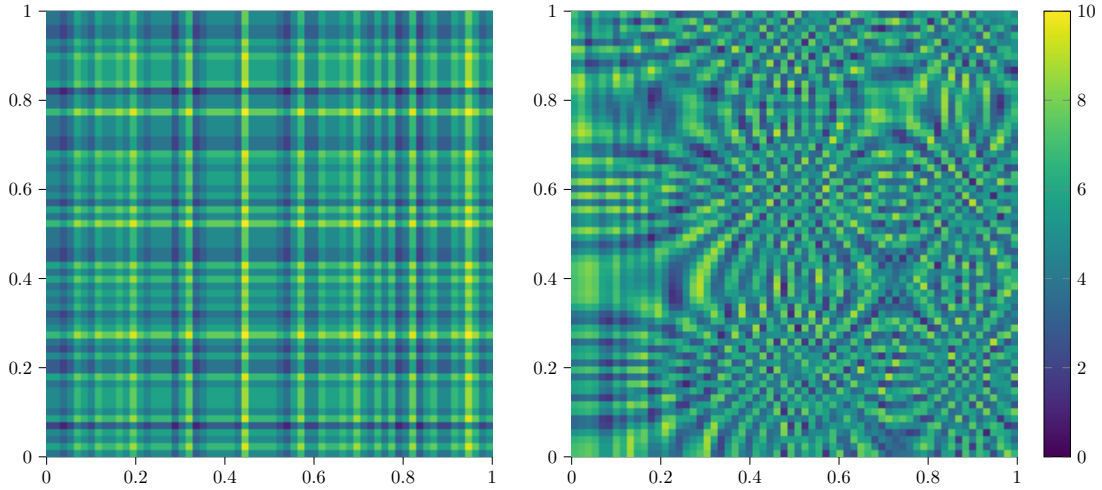


FIGURE 4.1. Coefficient A_1 (left) with values between 1 and 10 and coefficient A_2 (right) with values between 1 and 9. Both coefficients vary on the scale $\varepsilon = 2^{-6}$.

Remark 3.14. If the source function f is smooth enough in space and time, i.e. $k \geq 2$, the critical term with the lowest order in the full error estimate is the term $H^{j+2} |\partial_t^2 u|_{H^{j+1}}$; cf. the last term in equation (3.26) estimated with (3.24). From Assumption 3.4, we know that $j \geq 0$ such that we get a convergence rate of at least order $r \geq 2$. In the case of rough L^∞ -coefficients, we cannot expect more than H^1 -regularity in space for the function $\partial_t^2 u$. That is, $r = 2$ is the highest possible rate under minimal assumptions on the coefficient. We note, however, that the constant in front of the H^2 -term scales like $C_{\text{pr}}^2 \lesssim (p+1)^{-2}$ such that we expect the error to be smaller even if the rate does not increase. This scaling is also observed in the numerical examples in Section 4. If the coefficient A is smoother, we may obtain higher regularity of $\partial_t^2 u$ and, thus, an increased convergence rate, which is then capped at $r = p+2$. Note that if the coefficient is smooth but still has multiscale features, then the higher rate generally cannot be observed, since the spatial derivatives scale negatively with ε if the coefficient varies on the scale ε . In the next section, we present several numerical examples which indicate the reduced order in the general L^∞ -setting and a higher order convergence for smooth and slowly oscillating coefficients.

Remark 3.15. Analogously to [Kar11], we may obtain an $L^\infty(0, T; L^2(\Omega))$ -error estimate that essentially reads

$$\max_{0 \leq n \leq N} \|\tilde{u}_H^n - u(t_n)\|_{L^2(\Omega)} \lesssim (H^{r+1} + \tau^s) C_{\text{data}}.$$

That is, compared to the $L^\infty(0, T; H^1(\Omega))$ -error estimate shown above we obtain an additional order in space with $r \leq p+2$, dependent on the regularity of f and $\partial_t^2 u$ with analogue argumentation as in Remark 3.14. Further, we have $s = 2$ if $\theta \neq \frac{1}{12}$ and $s = 4$ if $\theta = \frac{1}{12}$.

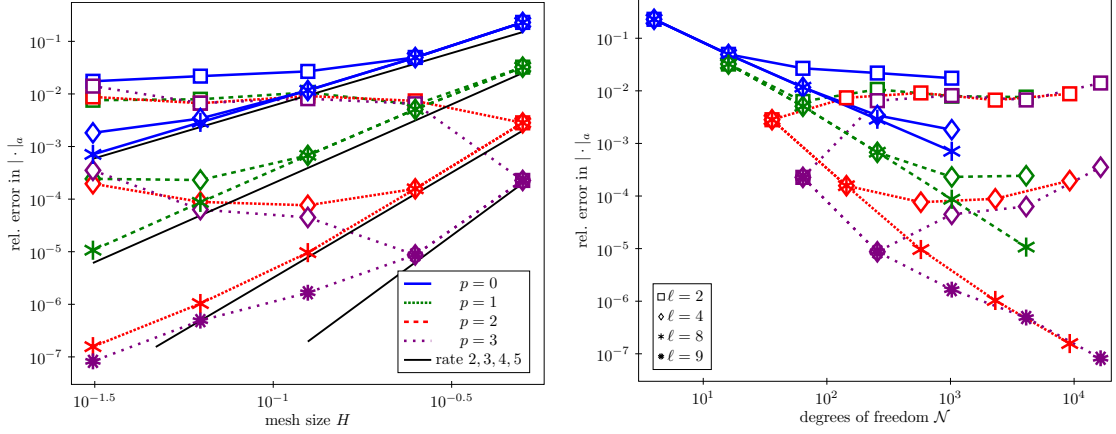


FIGURE 4.2. Relative $|\cdot|_a$ -errors for the coefficient A_1 with respect to the coarse mesh size H (left) and the degrees of freedom N (right) for different polynomial degrees p and localization parameters ℓ .

4. NUMERICAL EXAMPLES

In this section, we present several examples to verify the results presented in the previous sections. So far, we have assumed that the basis functions in \tilde{U}_H^ℓ can be computed exactly. This is not possible in practice since the corrector problems (2.9) are posed in infinite-dimensional spaces. Instead, we choose a finite element space $V_h \subset H_0^1(\Omega)$ and replace the space $H_0^1(\Omega)$ by V_h with mesh size $h \ll H$ in the above construction, which leads to error estimates with respect to a fine Galerkin finite element solution u_h instead of u with minor modifications in the above analysis. Roughly speaking, this also corresponds to a (fine enough) discretization \mathcal{C}_h^ℓ of the correction operator \mathcal{C}^ℓ . More details can be found in [Mai21, Sec. 4.3]. In the following, we therefore compute fully discrete p -LOD- θ solutions $\tilde{u}_{H,h}^{\ell,n} \in (1 - \mathcal{C}_h^\ell)U_H \subset V_h$ and compare the results to a reference Galerkin finite element approximation $u_h \in V_h$ of (2.2).

Throughout, we choose $\Omega = (0,1)^2$ with $T = 1$ and the two multiscale coefficients A_1 and A_2 shown in Figure 4.1, which both oscillate on the scale $\varepsilon = 2^{-6}$. The first coefficient A_1 takes values between 1 and 10 and the second coefficient A_2 varies between 1 and 9. The reference solution is computed on a mesh \mathcal{T}_h with mesh size $h = 2^{-8}$, and we measure the errors at the final time $T = 1$ in the norm $|\cdot|_a = \sqrt{a(\cdot, \cdot)}$ if not stated otherwise. In the plots, we show errors with respect to the mesh size H and the number of degrees of freedom N , respectively.

First example. For the first example, we prescribe homogeneous initial conditions $u_0 = v_0 = 0$, a right-hand side $f = \sin(\pi x_1) \sin(\pi x_2) \sin^4(t)$, and use the coefficient A_1 depicted in Figure 4.1 (left). We use the Crank–Nicolson scheme, i.e., $\theta = \frac{1}{4}$ for the time integration with a constant time step size $\tau = 2^{-9}$ for all p -LOD- θ solutions as well as the reference solution to investigate the spatial errors only. The results are plotted in Figure 4.2. In the left plot, we observe a convergence rate of at least two with respect to the mesh size H for each of the polynomial degrees, which is generally in line with the error analysis in the previous section. Moreover, we observe that the errors for $p = 1$ converge with order three, which is higher than expected, and even for $p = 2$ and larger values of H

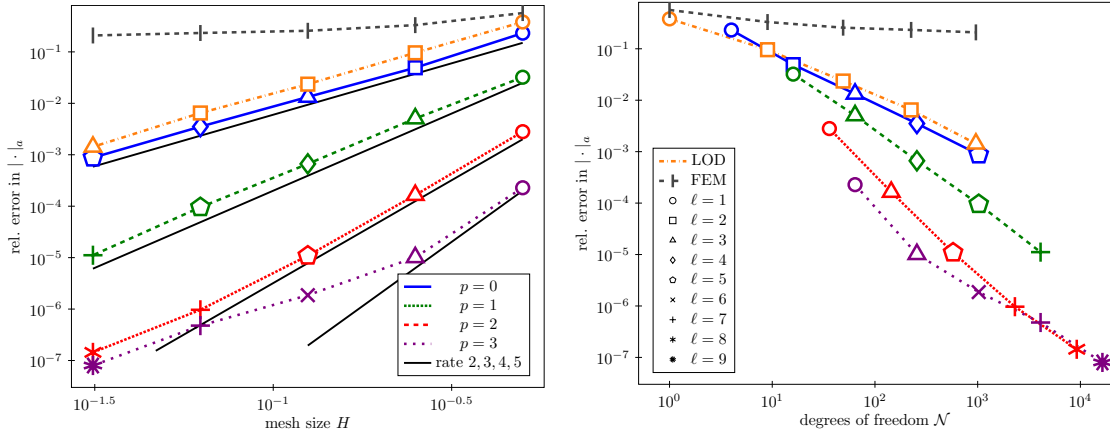


FIGURE 4.3. Relative $\|\cdot\|_a$ -errors for the second example with respect to the coarse mesh size H (left) and the number of degrees of freedom N (right) for different polynomial degrees p and localization parameters ℓ .

a higher order rate can be observed. This may be explained by the fact that the term that leads to the (reduced) second order convergence is of lower magnitude such that its effect is only observed for smaller values of the error, where the reduced rate is clearly visible. We emphasize that the observed reduction of the convergence rate is not related to the localization error as it persists also when increasing ℓ . In the right plot, the error is depicted with respect to the number of degrees of freedom N and we observe that higher polynomial degrees overall lead to smaller errors such that moderately increasing the polynomial degree appears to be beneficial even if arbitrarily high orders of convergence cannot be expected. The reasoning for this observation is the scaling of the constants in the above error estimates, which scale like $(p+1)^{-2}$ (cf. Remark 3.14). Both plots in Figure 4.2 show that for a small localization parameter ℓ , especially with higher polynomial degrees p , the error stagnates with decreasing mesh size, which is related to the regimes where the localization error dominates. In order to increase visibility of further plots, we omit all lines with a small localization parameter and instead indicate with the marker which localization is needed for each polynomial degree and mesh size. This also makes sense as in practice one would choose the lowest possible localization that still yields the desired convergence behavior.

Second example. In Figure 4.3, we show the errors of a second example based on the coefficient A_2 depicted in Figure 4.1 (right) as well as the initial conditions, the right-hand side, and the fine discretization parameters h and τ as in the first example. In particular, we present the behavior of the p -LOD- θ method with $\theta = \frac{1}{4}$ (Crank–Nicolson scheme) and compare it with other spatial discretization approaches, namely the classical FEM and the original first-order LOD method. We observe that the errors of the FEM are in the pre-asymptotic regime, where the mesh size H does not resolve the oscillation scale ε and the FEM solution fails to approximate the solution. The LOD method as used in [AH17] converges with order two, and the size of the errors are comparable to the errors of the p -LOD- θ method with polynomial degree $p = 0$. From Figure 4.3 (right), we particularly observe that much lower errors with respect to the number of degrees of freedom compared to the original LOD method can be achieved by increasing the

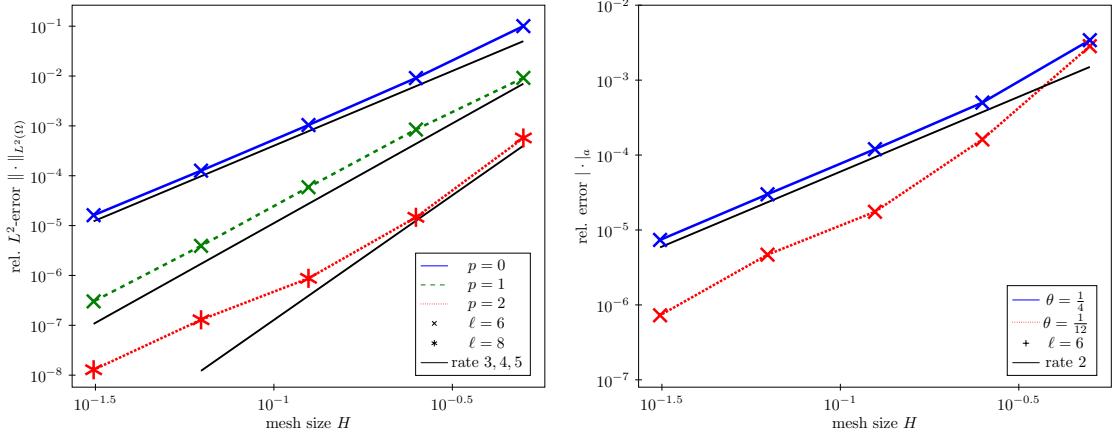


FIGURE 4.4. Relative L^2 -errors for the second example for $\theta = \frac{1}{12}$ (left) and relative $|\cdot|_a$ -errors for the second example for $\theta = \frac{1}{4}$ compared to $\theta = \frac{1}{12}$ for $p = 2$ (right) with time step sizes dependent on H and h , respectively.

polynomial degree. Analogously to above, we partially observe higher-order rates, which only for smaller magnitudes of the error are capped by two as predicted by the theory.

Since the convergence rates of the p -LOD- θ method are capped at $r = 2$ in the most general L^∞ -setting, a general question is whether a higher-order time discretization is useful in the first place. An illustration is given in Figure 4.4. The plot on the left shows the relative errors in the L^2 -norm in space. Here we choose $\theta = \frac{1}{12}$ with coarse time step sizes $\mathfrak{T} = 2^{-5}H$ and fine time step sizes $\tau = 2^{-5}h$ for the reference solution such that the CFL condition (3.3) holds. We observe convergence rates of one additional order compared to the errors measured in $|\cdot|_a$, see Remark 3.15 and Figure 4.3. The convergence rate for the Crank–Nicolson scheme in this example would be capped at $s = 2$ and the higher-order would not be observed. Figure 4.4 (right) gives another reason to why the choice $\theta = \frac{1}{12}$ can be better suited compared to other choices of θ . We choose both $\theta = \frac{1}{4}$ and $\theta = \frac{1}{12}$ and time step sizes that depend on the mesh size, i.e., $\mathfrak{T} = 2^{-5}H$ and $\tau = 2^{-5}h$. We observe that for the Crank–Nicolson scheme the relative $|\cdot|_a$ -errors eventually hit the temporal error plateau. For the scheme with $\theta = \frac{1}{12}$ we do obtain smaller errors since the temporal error plateau is not reached.

Third example. In Figure 4.5, we show the errors of a third example involving a smooth coefficient $A_3(x) = 1 + \frac{1}{2} \sin(x_1) \sin(2x_2)$, the right-hand side $f = \sin^4(\pi x_1) \sin^4(\pi x_2) \sin^4(t)$, and homogeneous initial conditions $u_0 = v_0 = 0$. The depicted results are generally in line with Remark 3.14. More precisely, in this example we have additional regularity of u in space and time, in particular the scaling of H^j -norms of $\partial_t^2 u$ for some $j \in \mathbb{N}_0$ is not severe, since the coefficient only oscillates on a rather coarse scale. Based on Remark 3.14, convergence rates in space of order $r = p + 2$ can be expected. The plots in Figure 4.5 show the errors of the p -LOD- θ method with $\theta = \frac{1}{12}$, $\mathfrak{T} = 2^{-5}H$ and $\tau = 2^{-5}h$, and we observe the additional rates as expected from the theory, which are capped at 4 due to the temporal error.

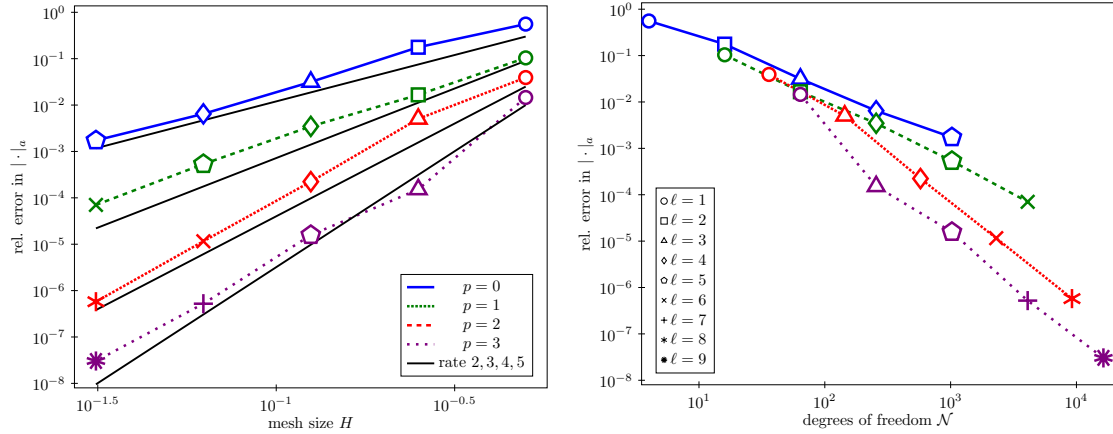


FIGURE 4.5. Relative $|\cdot|_a$ -errors for the third example with smooth coefficient and right-hand side for $\theta = \frac{1}{12}$ with respect to the coarse mesh size H (left) and the number of degrees of freedom \mathcal{N} (right) for different polynomial degrees p and localization parameters ℓ .

5. CONCLUSIONS

In this paper, we have presented a method to solve the acoustic wave equation with oscillating coefficients, where we combined a higher-order extension of the LOD method for the spatial discretization with the θ -scheme for time stepping. We have given rigorous a-priori error estimates and observed that arbitrarily high orders of convergence in space as in the elliptic case cannot be expected for the wave equation if only minimal assumptions on the coefficient hold. Nevertheless, our method can still achieve smaller errors by increasing the polynomial degree compared to lower-order approaches with a similar amount of degrees of freedom. This justifies a suitable increase of the polynomial degree. Further, if the coefficient is sufficiently smooth, higher-orders can be achieved.

Future research aims at modifying the presented approach to be better suited for an application to the heterogeneous wave equation. In particular, we aim at obtaining a truly higher-order method in space and time already under minimal assumptions on the coefficient.

ACKNOWLEDGMENTS

Funding from the Deutsche Forschungsgemeinschaft (DFG, German Research Foundation) – Project-ID 258734477 – SFB 1173 is gratefully acknowledged. We would also like to thank Moritz Hauck for fruitful discussions regarding the implementation of the method.

REFERENCES

- [AEEV12] A. Abdulle, W. E, B. Engquist, and E. Vanden-Eijnden. The heterogeneous multiscale method. *Acta Numer.*, 21:1–87, 2012.
- [AG11] A. Abdulle and M. J. Grote. Finite element heterogeneous multiscale method for the wave equation. *Multiscale Model. Simul.*, 9(2):766–792, 2011.
- [AH17] A. Abdulle and P. Henning. Localized orthogonal decomposition method for the wave equation with a continuum of scales. *Math. Comp.*, 86(304):549–587, 2017.

- [AHP21] R. Altmann, P. Henning, and D. Peterseim. Numerical homogenization beyond scale separation. *Acta Numer.*, 30:1–86, 2021.
- [AM17] M. Almqvist and M. Mehlin. Multilevel local time-stepping methods of Runge-Kutta-type for wave equations. *SIAM J. Sci. Comput.*, 39(5):A2020–A2048, 2017.
- [Chr09] S. H. Christiansen. Foundations of finite element methods for wave equations of Maxwell type. In *Applied wave mathematics*, pages 335–393. Springer, Berlin, Heidelberg, 2009.
- [Cia78] P. G. Ciarlet. *The Finite Element Method for Elliptic Problems*. North-Holland, Amsterdam, 1978.
- [DHM23] Z. Dong, M. Hauck, and R. Maier. An improved high-order method for elliptic multiscale problems. *SIAM J. Numer. Anal.*, 61(4):1918–1937, 2023.
- [EE03] W. E and B. Engquist. The heterogeneous multiscale methods. *Commun. Math. Sci.*, 1(1):87–132, 2003.
- [EE05] W. E and B. Engquist. The heterogeneous multi-scale method for homogenization problems. In *Multiscale methods in science and engineering*, volume 44 of *Lect. Notes Comput. Sci. Eng.*, pages 89–110. Springer, Berlin, Heidelberg, 2005.
- [EHR11] B. Engquist, H. Holst, and O. Runborg. Multi-scale methods for wave propagation in heterogeneous media. *Commun. Math. Sci.*, 9(1):33–56, 2011.
- [Eva10] L. C. Evans. *Partial Differential Equations*, volume 19 of *Graduate Studies in Mathematics*. American Mathematical Society, Providence, RI, second edition, 2010.
- [Geo03] E. H. Georgoulis. *Discontinuous Galerkin methods on shape-regular and anisotropic meshes*. PhD thesis, University of Oxford, 2003.
- [GLM23] M. Görtz, P. Ljung, and A. Målqvist. Multiscale methods for solving wave equations on spatial networks. *Comput. Methods Appl. Mech. Engrg.*, 410:Paper No. 116008, 24, 2023.
- [GM23] S. Geever and R. Maier. Fast mass lumped multiscale wave propagation modelling. *IMA J. Numer. Anal.*, 43(1):44–72, 2023.
- [GMM15] M. J. Grote, M. Mehlin, and T. Mitkova. Runge-Kutta-based explicit local time-stepping methods for wave propagation. *SIAM J. Sci. Comput.*, 37(2):A747–A775, 2015.
- [HFMQ98] T. J. R. Hughes, G. R. Feijóo, L. Mazzei, and J.-B. Quincy. The variational multiscale method – a paradigm for computational mechanics. *Comput. Methods Appl. Mech. Engrg.*, 166(1-2):3–24, 1998.
- [HP13] P. Henning and D. Peterseim. Oversampling for the multiscale finite element method. *Multiscale Model. Simul.*, 11(4):1149–1175, 2013.
- [HP22] M. Hauck and D. Peterseim. Multi-resolution localized orthogonal decomposition for Helmholtz problems. *Multiscale Model. Simul.*, 20(2):657–684, 2022.
- [HSS02] P. Houston, C. Schwab, and E. Süli. Discontinuous *hp*-finite element methods for advection-diffusion-reaction problems. *SIAM J. Numer. Anal.*, 39(6):2133–2163, 2002.
- [Hug95] T. J. R. Hughes. Multiscale phenomena: Green’s functions, the Dirichlet-to-Neumann formulation, subgrid scale models, bubbles and the origins of stabilized methods. *Comput. Methods Appl. Mech. Engrg.*, 127(1-4):387–401, 1995.
- [JE12] L. Jiang and Y. Efendiev. A priori estimates for two multiscale finite element methods using multiple global fields to wave equations. *Numer. Methods Partial Differential Equations*, 28(6):1869–1892, 2012.
- [JEG10] L. Jiang, Y. Efendiev, and V. Ginting. Analysis of global multiscale finite element methods for wave equations with continuum spatial scales. *Appl. Numer. Math.*, 60(8):862–876, 2010.
- [Jol03] P. Joly. Variational methods for time-dependent wave propagation problems. In *Topics in computational wave propagation*, volume 31 of *Lect. Notes Comput. Sci. Eng.*, pages 201–264. Springer, Berlin, Heidelberg, 2003.
- [Kar11] S. Karaa. Finite element θ -schemes for the acoustic wave equation. *Adv. Appl. Math. Mech.*, 3:181–203, 04 2011.
- [KL07] S. Kim and H. Lim. High-order schemes for acoustic waveform simulation. *Appl. Numer. Math.*, 57(4):402–414, 2007.
- [KM06] O. Korostyshevskaya and S. E. Minkoff. A matrix analysis of operator-based upscaling for the wave equation. *SIAM J. Numer. Anal.*, 44(2):586–612, 2006.
- [LKD07] H. Lim, S. Kim, and J. Douglas, Jr. Numerical methods for viscous and nonviscous wave equations. *Appl. Numer. Math.*, 57(2):194–212, 2007.

- [LM72] J.-L. Lions and E. Magenes. *Non-homogeneous boundary value problems and applications. Vol. I*, volume Band 181 of *Die Grundlehren der mathematischen Wissenschaften*. Springer-Verlag, New York-Heidelberg, 1972. Translated from the French by P. Kenneth.
- [LMP21] P. Ljung, A. Målqvist, and A. Persson. A generalized finite element method for the strongly damped wave equation with rapidly varying data. *ESAIM Math. Model. Numer. Anal.*, 55(4):1375–1403, 2021.
- [Mai20] R. Maier. *Computational Multiscale Methods in Unstructured Heterogeneous Media*. PhD thesis, University of Augsburg, 2020.
- [Mai21] R. Maier. A high-order approach to elliptic multiscale problems with general unstructured coefficients. *SIAM J. Numer. Anal.*, 59(2):1067–1089, 2021.
- [MP14] A. Målqvist and D. Peterseim. Localization of elliptic multiscale problems. *Math. Comp.*, 83(290):2583–2603, 2014.
- [MP19] R. Maier and D. Peterseim. Explicit computational wave propagation in micro-heterogeneous media. *BIT Numer. Math.*, 59(2):443–462, 2019.
- [MP20] A. Målqvist and D. Peterseim. *Numerical homogenization by localized orthogonal decomposition*, volume 5 of *SIAM Spotlights*. Society for Industrial and Applied Mathematics (SIAM), Philadelphia, PA, 2020.
- [MV22] B. Maier and B. Verfürth. Numerical upscaling for wave equations with time-dependent multiscale coefficients. *Multiscale Model. Simul.*, 20(4):1169–1190, 2022.
- [New59] N. M. Newmark. A method of computation for structural dynamics. *J. Eng. Mech. Div.*, 85(3):67–94, 1959.
- [OS19] H. Owhadi and C. Scovel. *Operator-adapted wavelets, fast solvers, and numerical homogenization*, volume 35 of *Cambridge Monographs on Applied and Computational Mathematics*. Cambridge University Press, Cambridge, 2019.
- [Owh17] H. Owhadi. Multigrid with rough coefficients and multiresolution operator decomposition from hierarchical information games. *SIAM Rev.*, 59(1):99–149, 2017.
- [OZ08] H. Owhadi and L. Zhang. Numerical homogenization of the acoustic wave equations with a continuum of scales. *Comput. Methods Appl. Mech. Engrg.*, 198(3–4):397–406, 2008.
- [OZ17] H. Owhadi and L. Zhang. Gamblets for opening the complexity-bottleneck of implicit schemes for hyperbolic and parabolic ODEs/PDEs with rough coefficients. *J. Comput. Phys.*, 347:99–128, 2017.
- [PS17] D. Peterseim and M. Schedensack. Relaxing the CFL condition for the wave equation on adaptive meshes. *J. Sci. Comput.*, 72(3):1196–1213, 2017.
- [Sch98] C. Schwab. *p- and hp-finite element methods. Theory and applications in solid and fluid mechanics*. Numerical Mathematics and Scientific Computation. The Clarendon Press, Oxford University Press, New York, 1998.
- [VMK05] T. Vdovina, S. E. Minkoff, and O. Korostyshevskaya. Operator upscaling for the acoustic wave equation. *Multiscale Model. Simul.*, 4(4):1305–1338, 2005.

APPENDIX A. ADDITIONAL REGULARITY

In this section, we provide the sufficient assumptions to obtain the higher regularity which is needed in Theorem 3.6 to enable higher-order convergence rates. Note that we need the coefficient A and also the boundary $\partial\Omega$ to be smooth enough and A not to have multiscale features, i.e., the coefficient may only oscillate on a rather coarse scale ε . This is due to the norms of the spatial derivatives of the solution scaling negatively with ε . We fix $k, j \in \mathbb{N}$ with $k \geq j + 2$ and introduce a stricter version of Assumption 3.4.

Assumption A.1. Assume that

- (B0) $f \in C^4([0, T]; H^k(\Omega))$, $u(0) = u_0 \in H^{j+3}(\Omega)$, $\partial_t u(0) = v_0 \in H^{j+2}(\Omega)$,
- (B1) $u_0 \in H_0^1(\Omega)$, $v_0 \in H_0^1(\Omega)$,
- (B2) $\partial_t^m u(0) := \partial_t^{m-2} f(0) + \operatorname{div} A \nabla (\partial_t^{m-2} u(0)) \in H_0^1(\Omega)$, for $m = 2, \dots, \max\{4, j + 2\}$,
- (B3) $\partial_t^n u(0) := \partial_t^{n-2} f(0) + \operatorname{div} A \nabla (\partial_t^{n-2} u(0)) \in L^2(\Omega)$, for $n = \max\{5, j + 3\}$,

(B4) there exists a constant $C_{\text{init}} > 0$ such that

$$\|u_0\|_{H^{j+3}(\Omega)} + \|v_0\|_{H^{j+2}(\Omega)} + \sum_{m=2}^{\max\{4, j+2\}} \|\partial_t^m u(0)\|_{H_0^1(\Omega)} + \|\partial_t^n u(0)\|_{L^2(\Omega)} \leq C_{\text{init}},$$

With similar arguments as in [Eva10, Sec. 7.2] we then obtain under sufficient smoothness assumptions on A and $\partial\Omega$ that

$$u \in C^m([0, T]; H^{j+3-m}(\Omega)), \quad m = 0, \dots, j+3,$$

We can bound the norms of u by the right-hand side and initial conditions as follows. Let $C_{\text{data}}(j, k, \varepsilon) > 0$ be a generic constant that depends on the regularity parameters j, k and possibly on the oscillation scale ε . Note that the case $j = 0$ is covered by Assumption 3.4. For $j \geq 1$, we assume additionally that $k \geq j + 2$ and that Assumption A.1 holds. We then estimate

$$\begin{aligned} & \sum_{m=0}^4 \|\partial_t^m u\|_{C([0, T]; H_0^1(\Omega))} + \|\partial_t^5 u\|_{C([0, T]; L^2(\Omega))} \\ & \lesssim_\varepsilon \|f\|_{C^4([0, T]; H^k(\Omega))} + C_{\text{init}} \leq C_{\text{data}}(0, k, \varepsilon), \\ & \sum_{m=0}^3 \|\partial_t^m u\|_{C([0, T]; H^{j+3-m}(\Omega))} + \|\partial_t^4 u\|_{C([0, T]; H_0^1(\Omega))} + \|\partial_t^5 u\|_{C([0, T]; L^2(\Omega))} \\ & \lesssim_\varepsilon \|f\|_{C^4([0, T]; H^k(\Omega))} + C_{\text{init}} \leq C_{\text{data}}(j, k, \varepsilon), \quad j = 1, \\ & \sum_{m=0}^{j+3} \|\partial_t^m u\|_{C([0, T]; H^{j+3-m}(\Omega))} \lesssim_\varepsilon \|f\|_{C^4([0, T]; H^k(\Omega))} + C_{\text{init}} \leq C_{\text{data}}(j, k, \varepsilon), \quad j > 1. \end{aligned}$$

In the above equations we use \lesssim_ε to indicate an ε -dependence in the hidden constants. In our specific setting, the constants scale like negative powers of ε , such that we not only need the coefficient to be smooth but also to oscillate on rather coarse scales for the constant C_{data} to be reasonably bounded.

[†] INSTITUTE FOR APPLIED AND NUMERICAL MATHEMATICS, KARLSRUHE INSTITUTE OF TECHNOLOGY, ENGLERSTR. 2, 76131 KARLSRUHE, GERMANY

Email address: {felix.krumbiegel, roland.maier}@kit.edu